A T_1 Spin–Lattice Relaxation and a Cross-Polarization Dynamics Study of the Molecular Motions of a Side-Chain Liquid Crystalline Polymer

Regan L. Silvestri and Jack L. Koenig*

Department of Macromolecular Science, Case Western Reserve University, Cleveland, Ohio 44106

Received August 13, 1991; Revised Manuscript Received January 13, 1992

ABSTRACT: The local molecular dynamics of a side-chain liquid crystalline polymer were studied by ^{13}C nuclear magnetic resonance (NMR) spectroscopy relaxation experiments. The polymer liquid crystal (PLC) studied contains the 4-hydroxy-4′-methoxy-α-methylstilbene mesogen attached through a flexible spacer of three methylenic units to a poly(methyl acrylate) backbone. T_1 was determined as a function of temperature throughout the glassy and smectic states. Within the glassy state the mobility of all spins increased continuously with temperature due to thermal motions. The mobility then increased discontinuously at the glass to smectic transition. Activation energies for reorientation calculated from Arrhenius plots showed that the α spacer carbon is nearly as rigid as the mesogen. In contrast, the β spacer carbon is nearly 2 orders of magnitude more mobile. A study of the cross-polarization dynamics showed no significant trend in the parameters T_{CH} and $T_{1/2}$ as a function of temperature. Also, comparison of the relative values of $T_{1/2}$ at a given temperature showed no apparent difference between the mobilities of the three methylenic spacer carbons.

I. Introduction

Polymer liquid crystals (PLCs) are unique materials that combine the anisotropic ordering properties of a liquid crystal with the characteristic properties of a polymer. One approach in the successful development of PLCs has been the synthesis of side-chain polymer liquid crystals.

Dynamic problems existing in the successful development of useful PLCs makes them an interesting system to be studied. Solid-state ^{13}C nuclear magnetic resonance (NMR) spectroscopy is sensitive to local molecular dynamics over a wide range of motional frequencies varying from 10^2 to 10^{11} Hz.[1-3]

T_1 Inversion–Recovery. The method of inversion–recovery is used to measure the spin–lattice relaxation time constant T_1. For the cross-polarization-enhanced T_1 pulse sequence used (Figure 1B), the loss of magnetization, $M(t)$, as a function of the variable delay time, t, is described by a single-exponential decay

$$M(t) = M_0[e^{-t/T_1}] \quad (1)$$

where M_0 is the inherent total magnetization in the absence of relaxation effects and T_1 is the time constant defining the rate of the exponential decay (see Figure 2).[4]

Commonly, single-exponential decays are not observed.[1,5,6] In such cases, the data must be fit to a two-component or double-exponential decay

$$M(t) = M_0[x_s e^{-t/T_{1s}} + x_l e^{-t/T_{1l}}] \quad (2)$$

where x_s is the fraction of the inherent total magnetization that is due to the decay process with a short time constant T_{1s} and x_l is the fraction of the inherent total magnetization that is due to the decay process with a long time constant T_{1l}.

The fractions of the two components sum to one

$$x_s + x_l = 1 \quad (3)$$

Substitution of eq 3 into eq 2 allows eq 2 to be written

$$M(t) = M_0[x_s e^{-t/T_{1s}} + (1 - x_s)e^{-t/T_{1l}}] \quad (4)$$

in terms of one less parameter.

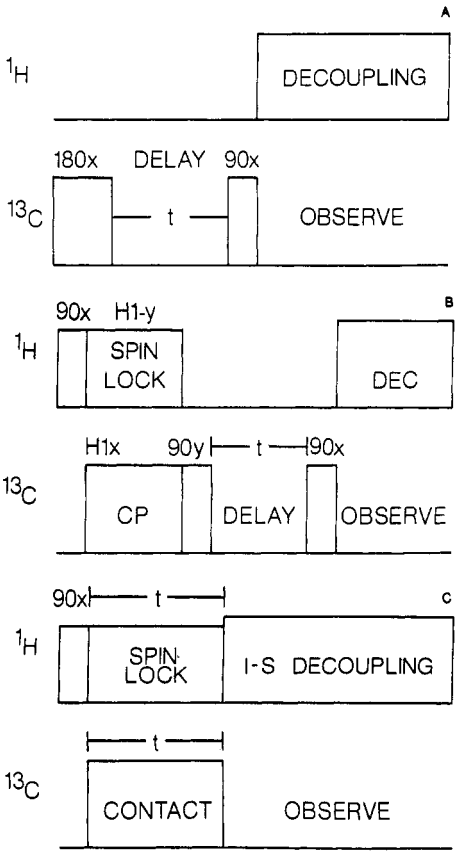

Figure 1. ^{13}C NMR pulse sequences for (A) T_1 inversion–recovery, (B) CP T_1 inversion–recovery, and (C) cross-polarization with a variable contact time.

During the variable recovery time, molecular motions cause lattice fluctuations that stimulate relaxation. The magnetization precesses in the static magnetic field and couples effectively with lattice motions of a similar frequency. Thus, T_1 is sensitive to molecular motions in the MHz frequency regime.[1,7,8] Short-range localized motions of molecular groups occur in the MHz frequency regime.[7,9] Common fast motions are internal reorientations (such as trans–gauche isomerizations or ring flips).[10]

0024-9297/92/2225-2341$03.00/0

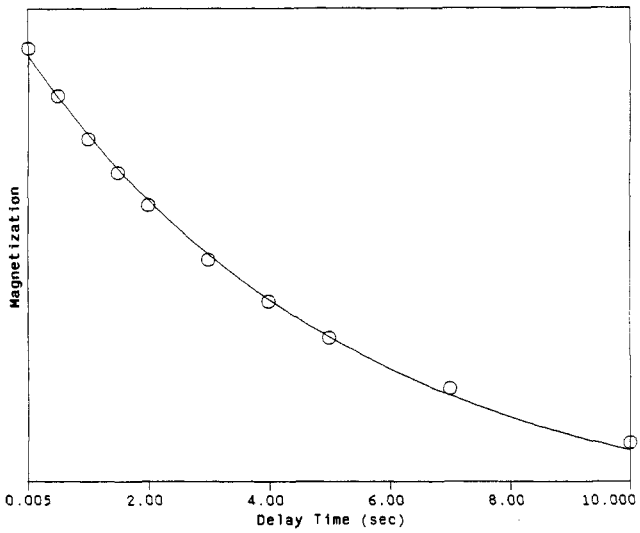

Figure 2. Plot of the magnetization as a function of the variable delay time in a CP T_1 experiment for the peak at 45 ppm that has been assigned to the quaternary carbon in the backbone, C_b.

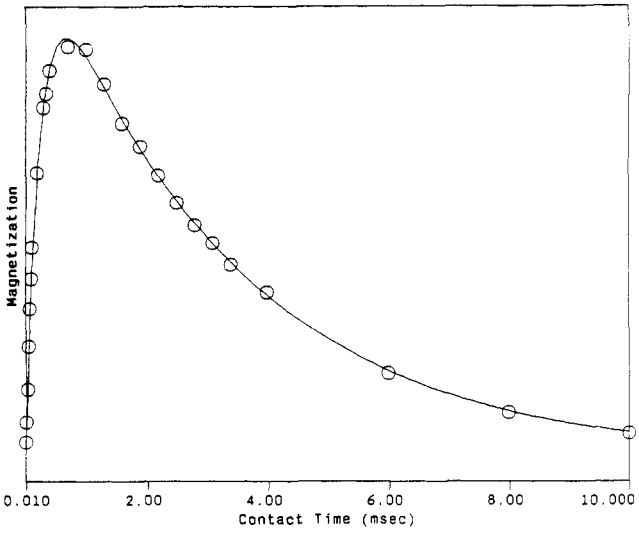

Figure 3. Plot of the magnetization as a function of the variable contact time in a cross-polarization with variable contact time experiment for the peak at 45 ppm that has been assigned to the quaternary carbon in the backbone, C_b.

This motional frequency regime is studied herein because these high-frequency intramolecular motions can be characteristic of rigid mesogenic cores.[2,9,11] Also, this motional regime is studied herein because glassy polymers typically undergo motions that are limited to a local area.

Cross-Polarization Dynamics. The cross-polarization (CP) with variable contact time pulse sequence (Figure 1C) is used to measure the time constants T_{CH} and ^1H $T_{1\rho}$ (also written T_{HH}). In the cross-polarization with variable contact time experiment, the magnetization is described by

$$M(t) = M_0[e^{-t/T_{HH}} - e^{-t/T_{CH}}]\{T_{HH}/(T_{HH} - T_{CH})\} \quad (5)$$

where M_0 is the inherent total magnetization in the absence of relaxation effects (see Figure 3).[7] The exponential decay with a time constant T_{HH} describes the decay of the spin-locked ^1H nuclei in the rotating frame. The exponential increase with a time constant T_{CH} describes the transfer of polarization from the abundant ^1H spin reservoir to the dilute ^{13}C spin reservoir.[7]

The ^1H $T_{1\rho}$ process is dominated by spin diffusion such that motional information is lost.[12] However, the time constant T_{CH} can be characteristic of molecular motions. Rigid carbons spin lock efficiently so the transfer of polarization occurs quickly. Therefore, the time constant T_{CH} is short for rigid carbons.[9]

For methylene and methine carbons there are two mechanisms for the buildup of cross-polarized magnetization.[13] The result is the observation of two T_{CH}s: one for the initial process and one for the final. Accounting for the two processes, eq 5 becomes

$$M(t) = M_0'[e^{-t/T_{HH}} - x_s e^{-t/T_{CHs}} - x_l e^{-t/T_{CHl}}] \quad (6)$$

where T_{CHs} in the short time constant for the initial or coherent process and T_{CHl} is the long time constant for the second process. Likewise, x_s is the fraction of the total buildup of magnetization due to the process with a short time constant, and x_l is the fraction of the total buildup of magnetization due to the process with a long time constant. Furthermore, M_0' also contains the term $\{T_{HH}/(T_{HH} - T_{CH})\}$.

The fractions of the short and long components sum to one (eq 3) so eq 6 can be written

$$M(t) = M_0'[e^{-t/T_{HH}} - x_s e^{-t/T_{CHs}} - (1 - x_s)e^{-t/T_{CHl}}] \quad (7)$$

in terms of one less variable.

As an alternative to T_{CH}, the time constant $T_{1/2}$ can be used to describe the buildup of magnetization.[13] $T_{1/2}$ is one-half of the time it takes for the cross-polarized magnetization to reach its maximum intensity before ^1H $T_{1\rho}$ effects cause a decay in the magnetization. As such, a short $T_{1/2}$ indicates a rigid system that cross-polarizes quickly.[9]

$T_{1/2}$ is useful for describing methylene and methine carbons because a single T_{CH} cannot be calculated.[9,13] The rigidity of a carbon is reflected by the coherent or initial process (T_{CHs}).[13] However, $T_{1/2}$ is used to describe mobility to avoid weighting problems between the relative proportions of the two processes.

T_{CH} (or its equivalent representation as $T_{1/2}$) is a quantitative measure of the efficiency of the cross-polarization process for a spin. During cross-polarization, carbon magnetization is achieved by the transfer from polarized protons via the static dipolar interaction between the two nuclei.[14] Thus, T_{CH} (and its equivalent representation as $T_{1/2}$) is sensitive to near static motions in the low Hz frequency range.[9]

The transfer of CP magnetization occurs in the presence of a radio-frequency (rf) spin-locking pulse. The power of a typical rf pulse creates an effective field that causes the spins to precess with a frequency on the order of a few tens of kHz. When the static dipolar interaction is partially averaged by this kHz motion, the transfer of magnetization becomes less efficient.[13] That is, T_{CH} becomes larger when there is more kHz motion. Consequently, T_{CH} is also sensitive to molecular motions in the kHz frequency regime.[9,15,16]

The kHz frequency regime is often used to describe the dynamics of rigid solids and viscous polymer backbones.[1,7] That is, high-viscosity polymers typically have relatively slow (low frequency) motions in the kHz regime. Schaefer et al.[14] were able to unambiguously interpret relaxation data in the mid-kHz regime solely in terms of the main- and side-chain motions of glassy polymers in the solid state. In fact, a previous study of cross-polarization dynamics showed that poly(methyl methacrylate) had segmental motions with correlation frequencies on the order of 10 kHz.[14] This prompted the study herein since the side-chain PLC of interest is based on a poly(methyl methacrylate) backbone.

The Hz frequency regime describes slow, collective motions of entire groups of mesogens.[9,10] Coupled molecular groups such as liquid crystals exhibit such large-scale motions. For PLCs, it is also possible for small-scale motions such as ring flips to occur with such exceptionally low frequencies. Internal reorientations such as ring flips typically occur at high frequencies in the MHz regime. However, for PLCs the tight mesomorphic packing can slow ring flip motions to lower frequencies. Deuterium line shape analysis, sensitive to Hz motions, is commonly used to describe the molecular motions occurring in PLCs. This also prompted the study herein since T_{CH} is sensitive to Hz frequency regime molecular motions.

II. Experimental Section

Relaxation Measurements. Shown below is the side-chain PLC synthesized by Percec and Tomazos and studied herein.[17]

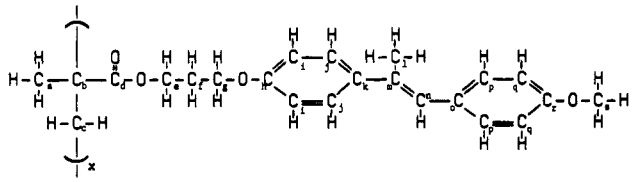

This PLC is termed 4′-3-PMA, where 4′ specifies the 4-hydroxy-4′-methoxy-α-methylstilbene mesogen, PMA specifies that poly(methyl acrylate) is the main-chain polymer backbone, and 3 specifies that the mesogen is connected to the backbone via a flexible free spacer of 3 methylenic units.

The inversion–recovery pulse sequence (Figure 1B) was used to determine the ^{13}C T_1 spin–lattice relaxation time, and the cross-polarization with variable contact time pulse sequence (Figure 1C) was used to determine the time constants T_{CH} and ^1H $T_{1\rho}$. The time constants were determined in the solid state at various temperatures ranging from 22 to 79 °C. The experiments were carried out on a Bruker MSL 300 spectrometer at a ^{13}C measuring frequency of 75.47 MHz and on a Nicolet NT 150 spectrometer at a ^{13}C measuring frequency of 37.73 MHz.

All experiments were carried out with gated high-powered dipolar decoupling (GHPD) and magic angle spinning (MAS) at 3 kHz. T_1 was determined with[4] and without cross-polarization (CP) signal enhancement (Figure 1A,B). The spin-looking contact time for cross-polarization was ~1 ms. The delay between pulse sequence repetitions was 4 s. It was not necessary to wait several carbon T_1 values to reestablish an equilibrium carbon magnetization, since a cross-polarization-enhanced pulse sequence was used for inversion–recovery. The rf fields were typically 50–70 kHz.

On the Bruker MSL 300 typically 800–1000 scans were signal averaged for each τ, and on the Nicolet NT 150 some 16 000 scans were signal averaged for each τ. For the inversion–recovery experiments, 6–12 variable delays were used ranging from 5 ms to 10 s. For the variable contact time experiments, 19–25 variable times were used ranging from 10 μs to 10 ms.

For the Bruker MSL 300, 7-mm-diameter zirconia rotors with Kel-F caps were used. For the Nicolet NT 150, pressed Al_2O_3 rotors with Kel-F caps were used. The chemical shift scale was set using adamantane. The magic angle was set by maximizing the peak intensities of KBr. The 90° pulse length was determined from null intensities of adamantane at 360° and 720°. The Hartmann–Hahn match was set by maximizing the peak intensities of adamantane in a cross-polarization experiment with a 3-ms contact pulse. Free induction decays (fids) with ~512W data points were collected and zero-filled to 8K data points before Fourier transformation.

Calculation of Relaxation Parameters. The appropriate exponential equations were least squares curve fit to the peak intensities on a MicroVax II using a general nonlinear least squares curve fitting program written in Fortran 77. Peak intensities were measured without baseline correction.[9]

To decide when two T_1s were necessary, successive variable delay times were included in a curve fit to a single exponential, and the standard deviation was monitored. When the data points fit properly to a single exponential, including the next data point in a curve fit to a single exponential increased the standard deviation of the fit by less than 5%. When the inclusion of the next successive point in the curve fit to a single exponential increased the standard deviation by more than 20%, then two T_1s were necessary. Analogous criterion were used to determine when two T_{CH}s were necessary.

Calculation of T_1. When two T_1s are observed, curve fitting eq 4 is difficult because four parameters (M_0, T_{1s}, T_{1l}, and x_s) must be fit simultaneously. To ensure that the proper values are determined, the following procedure is used.

First, eq 8 was fit to the portion of the data points with long τs

$$M(t) = M_{0l}e^{-t/T_{1l}} \tag{8}$$

to determine an estimate of T_{1l}, the time constant for the long process, and of M_{0l}, the total inherent magnetization due to the long process. It is possible to ignore the short component of eq 4 at long τs because the short component describes a fast relaxation process that has already relaxed to nearly zero at longer τs. Next, these estimates for the long process are substituted into eq 9 and held constant

$$M(t) = M_{0s}e^{-t/T_{1s}} + M_{0l}e^{-t/T_{1l}} \tag{9}$$

as the curve is fit to the entire set of data points to determine estimates for T_{1s} and M_{0s}. Finally, the estimates of all four parameters, T_{1s}, T_{1l}, M_{0s}, and M_{0l}, are used as starting points for the initial iteration of a curve fit of eq 9 to fit all four parameters simultaneously. Note that eq 9 is equivalent to eq 4 because

$$x_s = M_{0s}/(M_{0s} + M_{0l}) \tag{10}$$

It is necessary to determine estimates to ensure that the four-parameter curve fit converges on the proper values. Also, it is necessary to fit all four parameters simultaneously so that contributions from all processes are accounted for at all variable times.[9]

Calculation of T_{CH} and $T_{1/2}$. When two T_{CH}s are observed, five parameters (M_0', T_{HH}, T_{CHs}, T_{CHl}, and x_s) must be fit simultaneously.

First, a single-exponential decay is fit to the final portion of the curve to determine an estimate of T_{HH}. This estimate of T_{HH} is substituted into eq 5 and held constant as the curve is fit to only the first few data points to determine an estimate of T_{CHs}. This assumes that the slow process (with a long time constant T_{CHl}) does not contribute significantly to the initial portion of the curve since there has not been enough time for the slow process to build up significant magnetization. Next, the estimates of T_{HH} and T_{CHs} are substituted into eq 7 and held constant as a curve fit determines estimates for T_{CHl}, x_s, and M_0'. Finally, the estimates of all five parameters are used as starting points for the initial iteration to fit all five parameters of eq 7 simultaneously.

Values of $T_{1/2}$ are calculated by determining the maximum value of this function and subsequently the variable contact time when the function has its maximum value. This contact time is then divided by one-half.

III. Results

Previously published differential scanning calorimetry (DSC) and gel permeation chromatography (GPC) data are given in Table I.[17] The glass to smectic transition (55 °C heating, 42 °C cooling) is not accompanied by an exotherm or endotherm. As a result, when cooling from the smectic to glass state, smectic ordering is retained but frozen in the glass state. Therefore, the glassy material is ordered. Further proof that the transition at 55 °C is a glass transition is provided by shear measurements.[17] Above this temperature the material shears, but below this temperature the material is frozen. The anisotropic textures and corresponding thermal transitions were observed via optical polarized microscopy with a hot

Table I
Transition Temperatures (°C), M_n, and M_w/M_n for the PLC 4′-3-PMA[a]

	heating	cooling
T_{g-s}	55	42
T_{s-n}	85	75
T_{n-i}	115	110

$M_n = 43.6 \times 10^3$; $M_w/M_n = 2.5$

[a] Reference 17. Transition temperatures determined by DSC with heating and cooling rates of 20 °C/min; M_n and M_w/M_n determined by GPC.

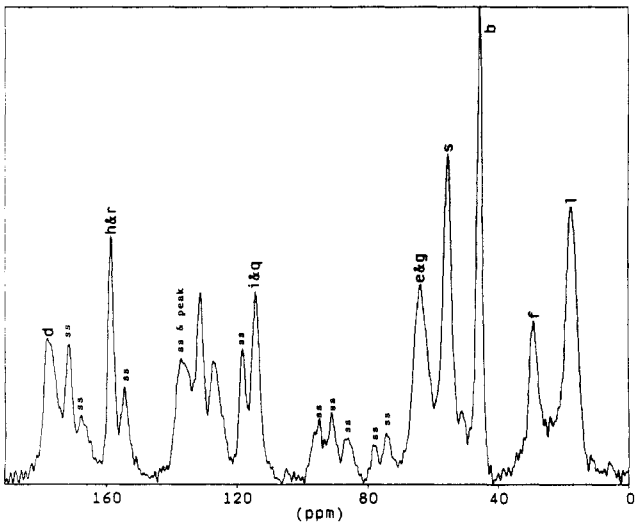

Figure 4. Cross-polarization/gated high-powered decoupling/magic angle spinning ^{13}C NMR spectrum with peak assignments of 4′-3-PMA at 300 MHz and 27 °C.

stage.[17] This furthered positive identification of the smectic to nematic and nematic to isotropic transitions.

Peak assignments are shown in Figure 4, where the letters correspond to the subscripted carbons as labeled in the chemical formula.[9] Spinning sidebands are labeled "ss".

Since T_g is a kinetically controlled process, the temperature at which T_g is observed is dependent on the motional frequency that the particular experimental technique observes.[9] Typically, the glass transition is shifted upward by 5–10 °C for each order of magnitude that the measurement frequency is increased.[8] DSC corresponds to measuring frequencies on the order of Hz. T_1 measures molecular motions in the MHz regime, and T_{CH} measures molecular motions in the Hz and kHz regimes.

Since unique T_1 values are obtained for each carbon, there is little ^{13}C spin diffusion.

Observation of Single/Double Exponentials for T_1. The fourth column of Table II lists values of T_1 at 27 °C measured using the cross-polarization-enhanced inversion–recovery pulse sequence shown in Figure 1B. Figure 2 is a typical plot of the decay of magnetization where a single-exponential decay (eq 1) is fit to the experimentally determined data points. Single-exponential decays are observed for each of the non-proton-bonded carbons C_b, C_d, C_h, and C_r. Note that only one value of T_1 is listed for each of these carbons in the fourth column of Table II. Double-exponential decays are observed for each of the proton-bonded carbons C_e, C_f, C_g, C_i, C_q, and C_s. Note that two T_1s are listed for each of these carbons.

The second and third columns of Table II list values of T_1 measured using the inversion–recovery pulse sequence without cross-polarization shown in Figure 1A. Single-exponential recoveries are observed for all carbons when this pulse sequence is used. Without cross-polarization, this pulse sequence is less sensitive and the long relaxation process is undetected.

Table II
Values of T_1 at 27 °C for the PLC 4′-3-PMA at (a) 150 MHz without Cross-Polarization, (b) 300 MHz without Cross-Polarization, and (c) 300 MHz with Cross-Polarization[a]

	GHPD 150 MHz	GHPD 300 MHz	CP/GHPD 300 MHz
C_b 45 ppm	3.39	5.54	5.68
C_d 177 ppm	very long	16.16	15.60
C_e and C_g 64 ppm	0.49	1.13	0.53 4.3
C_f 29 ppm	0.34	0.58	0.49 3.4
C_h and C_r 158 ppm	6.94	59.35	15.67
C_i and C_q 114 ppm	0.39	1.03	0.49 3.6
C_s 55 ppm	1.44	1.49	1.07 7.7

[a] The listing of two T_1s for a single carbon indicates a double exponential. Error: T_1, ± 0.07 s; T_{1s}, ± 0.09 s; T_{1l}, ± 0.4 s.

Temperature Dependence of T_1. T_1 was determined with cross-polarization signal enhancement at several temperatures ranging from 22 to 79 °C. Plots A–F of Figure 5 show T_1 as a function of temperature for the various carbons. When curve fitting to a biexponential decay is necessary, both T_1s are plotted at that temperature. The glass to smectic transition (T_{g-s}) is labeled on the temperature axes of Figure 5A–F.

Fast/Slow Motion Side of T_1 Minimum. To study molecular motions, T_1 values must be related to corresponding values of the rotational correlation time (τ_c). The rotational correlation time is the length of time that a molecule remains in a given state before the molecule reorients. As such, τ_c is a direct measure of the rate of motion.[9]

Because there is a minimum in the dependence of T_1 on τ_c, a given value of T_1 may correspond to either of two values for τ_c.[1,2] To determine which side of the minimum a relaxation occurs on, T_1 is determined at two static magnetic fields (B_0). T_1 is independent of B_0 on the fast or high-frequency side of the T_1 minimum; however, on the slow or low-frequency side of the T_1 minimum a lower value of T_1 is observed at lower static field strengths.[1,2,9,18]

Solid polymers, because of their high viscosity, usually undergo slow motions, i.e., motions on the slow side of the T_1 minimum. In the glassy state, solid polymers undergo particularly slow motions. Consequently, it is not surprising that C_b, C_e, C_g, C_f, C_h, C_r, C_i, and C_q undergo motions on the slow side of the T_1 minimum, as can be seen by comparing the lower values of T_1 at 150 MHz (second column of Table II) to the higher values of T_1 at 300 MHz (third column of Table II).

However, note in Table II that for the methoxy carbon (C_s) the same value of T_1 is observed at both 150 and 300 MHz. Therefore, the molecular motion that results in relaxation corresponds to the value of τ_c on the fast motion side of the minimum. C_s is a methyl carbon, so the motion is certainly rapid spinning of the methyl group about its C_3 axis. The third column of Table III lists which side of the T_1 minimum each relaxation is observed on.

Spin–Lattice Relaxation Mechanisms. Note that for the carbonyl carbon C_d a smaller value of T_1 is observed

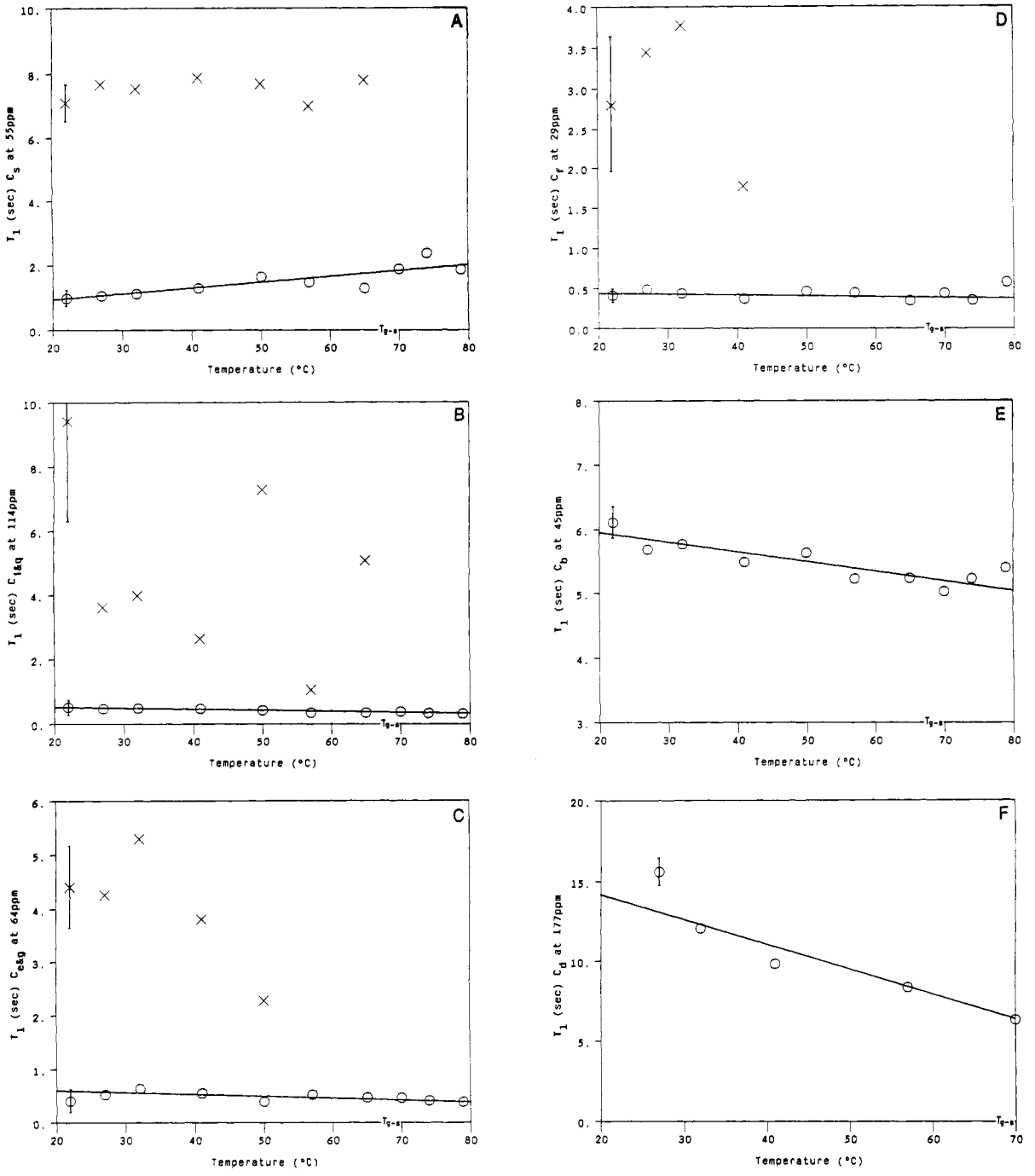

Figure 5. Plots of T_1, T_{1s}, and T_{1l} as a function of temperature for (A) the peak at 55 ppm assigned to C_s, (B) the peak at 114 ppm assigned to C_i and C_q, (C) the peak at 64 ppm assigned to C_e and C_g, (D) the peak at 29 ppm assigned to C_f, (E) the peak at 45 ppm assigned to C_b, and (F) the peak at 177 ppm assigned to C_d.

at a larger static magnetic field. The observation of a smaller T_1 at a larger field indicates relaxation by the chemical shift anisotropy (CSA) mechanism[9,18,19] instead of by the more common dipolar mechanism. At higher fields CSA is larger so relaxation by this mechanism is more efficient, resulting in a shorter T_1. This is a likely mechanism for the carbonyl carbon C_d because of the high anisotropy of a carbonyl group and because this carbon is not protonated so dipolar relaxation is inefficient.

The most common relaxation mechanism is dipole–dipole relaxation. Dipole–dipole relaxation occurs as a result of time fluctuations of the dipolar interaction and is a common mechanism due to the inherently strong nature of the dipolar interaction. The strength of the dipolar interaction is inversely related to the sixth power of r_{C-H}, the carbon to hydrogen internuclear distance (eq 11). Thus, if r_{C-H} is small, the dipolar interaction is strong and the resulting relaxation is efficient, or fast.

If a carbon is bound by a proton, r_{C-H} is the carbon to hydrogen bond length (regardless that the dipolar interaction is through space). Therefore, a bound proton ensures an extremely small r_{C-H} and subsequently an efficient or fast relaxation. Owing to this high efficiency, protonated carbons are nearly always relaxed via the dipole–dipole mechanism.[9,18-20] Dipole–dipole relaxation is the relaxation mechanism for the protonated carbons C_e, C_g, C_f, C_i, C_q, and C_s as listed in the second column of Table III.

For nonprotonated carbons, the dipolar relaxation mechanism is less efficient because the internuclear distance to nonbonded protons is larger.[9,18,19] Dipole–dipole relaxation via time fluctuations of the dipolar interaction

Table III
Mechanism by Which Relaxation Occurs in the Glassy State, the Location of the Motion Causing Relaxation with Respect to the T_1 Minimum, and τ_c Calculated from the Value of T_{1s} Determined by a Cross-Polarization-Enhanced Inversion-Recovery Experiment at 300 MHz and 27 °C

	relaxation mechanism	side of minimum	τ_c at 27 °C, s
C_b 45 ppm	dipolar: nonbonded protons	slow	n.a.
C_d 177 ppm	CSA	n.a.	n.a.
C_e and C_g 64 ppm	dipolar: bonded and nonbonded protons	slow	$(1.3 \pm 0.5) \times 10^{-6}$
C_f 29 ppm	dipolar: bonded and nonbonded protons	slow	$(1.2 \pm 0.4) \times 10^{-6}$
C_h and C_r 158 ppm	dipolar: nonbonded protons	slow	n.a.
C_i and C_q 114 ppm	dipolar: bonded and nonbonded protons	slow	$(5.8 \pm 0.9) \times 10^{-7}$
C_s 55 ppm	dipolar: bonded and nonbonded protons	fast	$(1.5 \pm 0.7) \times 10^{-11}$

between the carbon and nonbonded protons is the relaxation mechanism for the non-proton-bonded carbons C_b, C_h, and C_r (Table III).

Note in Table II that C_b, C_h, and C_r (dipolar relaxed via fluctuations of the weak dipolar interaction with nonbonded protons) have T_1s that are 5–10 times longer than C_e, C_g, C_f, C_i, and C_q (dipolar relaxed via fluctuations of the strong dipolar interaction with bonded protons). This demonstrates that dipolar relaxation is more efficient when a carbon has a bound proton. Also note in Table II that the CSA-relaxed carbonyl C_d has a longer T_1 than any other carbon due to the inefficiency of the CSA mechanism.

Cause of a Double Exponential for T_1. If there are two competing relaxation mechanisms with similar efficiencies, both mechanisms will act to relax the spin simultaneously. Each mechanism results in a decay with a characteristic time constant. This results in the observation of a two-component exponential decay. The fast process, characterized by T_{1s}, is dipolar relaxation as a result of fluctuations of the strong dipolar interaction with bound protons. The slow process, characterized by T_{1l}, is dipolar relaxation as a result of fluctuations of the weak dipolar interaction with nonbonded protons. Again, note that relaxation caused by fluctuations of the dipolar interaction with bound protons (corresponding to the short T_1) is faster because r_{C-H} is smaller.

In the glassy state double exponentials are observed for proton-bonded carbons, whereas in the smectic state single exponentials are observed. In the smectic state, sufficient mobility is introduced such that relaxation induced by fluctuations of the dipolar interaction with nonbonded protons does not occur. This constitutes a discontinuous increase in mobility at the glass to smectic transition.

The observation of double exponentials for semicrystalline polymers is commonly interpreted by assigning one relaxation process to the crystalline domains and the other relaxation process to the amorphous portion.[6] However, this is probably not the cause of a double exponential in this case because a single T_{HH} is observed, indicating that the PLC is likely composed of a single homogeneous phase to allow ^1H spin diffusion.[3,12]

Changes in Mobility with Temperature. The methoxy carbon C_s observed on the high-frequency or fast side of the T_1 minimum shows an increase in mobility with temperature. Figure 6A is a plot of T_{1s} as a function of temperature for the methoxy carbon C_s. Note that T_{1s} increases with an increase in temperature. Recall that the methoxy carbon was determined to undergo a fast motion on the high-frequency side of the T_1 minimum because the motion was rapid spinning of the methyl group. On the fast motion side of the T_1 minimum, an increase in T_1 moves to smaller values of τ_c, or shorter memory times.[1,2,9] Thus, the increase in T_{1s} with temperature represents an increase in the mobility of the methoxy carbon at higher temperatures. That is, the spinning of the methyl group about its axis is faster at higher temperatures. This gives little information about liquid crystalline dynamics. The methyl group could be rotating on a rigid crystalline core or on a flexible substituent, and the two could not be differentiated.

All of the carbons observed on the low-frequency or slow side of the T_1 minimum also show an increase in mobility with temperature. Plots B–D of Figure 6 show T_{1s} as a function of temperature for the protonated benzene carbons (C_i and C_q), the two outer methylene units of the spacer (C_e and C_g), and the center methylene unit of the spacer (C_f), respectively. Note that T_{1s} decreases at higher temperatures for these carbons. Note likewise in Figure 5E that T_1 also decreases with an increase in temperature for the quaternary carbon C_b. Recall that all of these carbons were determined to undergo slow motions on the low-frequency side of the T_1 minimum. On the slow side of the T_1 minimum a decrease in T_1 moves to smaller values of τ_c, or shorter memory times.[1,2,9] Therefore, the decrease in T_1 represents an increase in mobility at higher temperatures for these carbons.

In summary, there is a general trend for all carbons toward an increased mobility at higher temperatures.

Rotational Correlation Time. It has been established that mobility increases at higher temperatures for all carbons. Because various carbons increase mobility more than others, a comparison of the relative mobilities is desired. It is not possible to directly compare the relative rates of relaxation because different relaxation mechanisms have different inherent efficiencies and also because the number of bonded protons affects the relaxation rate of dipolar relaxed spins (eq 11). Instead, values of the rotational correlation time must be compared because τ_c is directly related to the rate of motion.

A theoretical model for dipolar relaxation can be used to calculate τ_c from T_1.[21] Assuming random isotropic reorientation of the C–H vector, τ_c is related to T_1 by

$$\frac{1}{NT_1} = \frac{1}{10}\frac{\gamma_H^2\gamma_C^2\hbar^2}{r_{C-H}^6}\{J_0(\omega_H-\omega_C) + 3J_1(\omega_C) + 6J_2(\omega_H+\omega_C)\} \quad (11)$$

where the spectral density function is

$$J(\omega) = \tau_c/(1 + \omega^2\tau_c^2) \quad (12)$$

Equation 11 must be solved numerically because the solution is field dependent.[1,2,9,21] The calculation of τ_c from T_1 simplifies on the fast side on the T_1 minimum to the linear equation

$$\frac{1}{NT_1} = \tau_c\frac{\gamma_H^2\gamma_C^2\hbar^2}{r_{C-H}^6} \quad (13)$$

where N is the number of bound protons and r_{C-H} is the internuclear carbon to hydrogen distance. Nevertheless, on the slow side of the T_1 minimum the general equation (eq 11) must be used.

The assumption of random isotropic rotation of the C–H vector can be crude for polymers. There are constraints

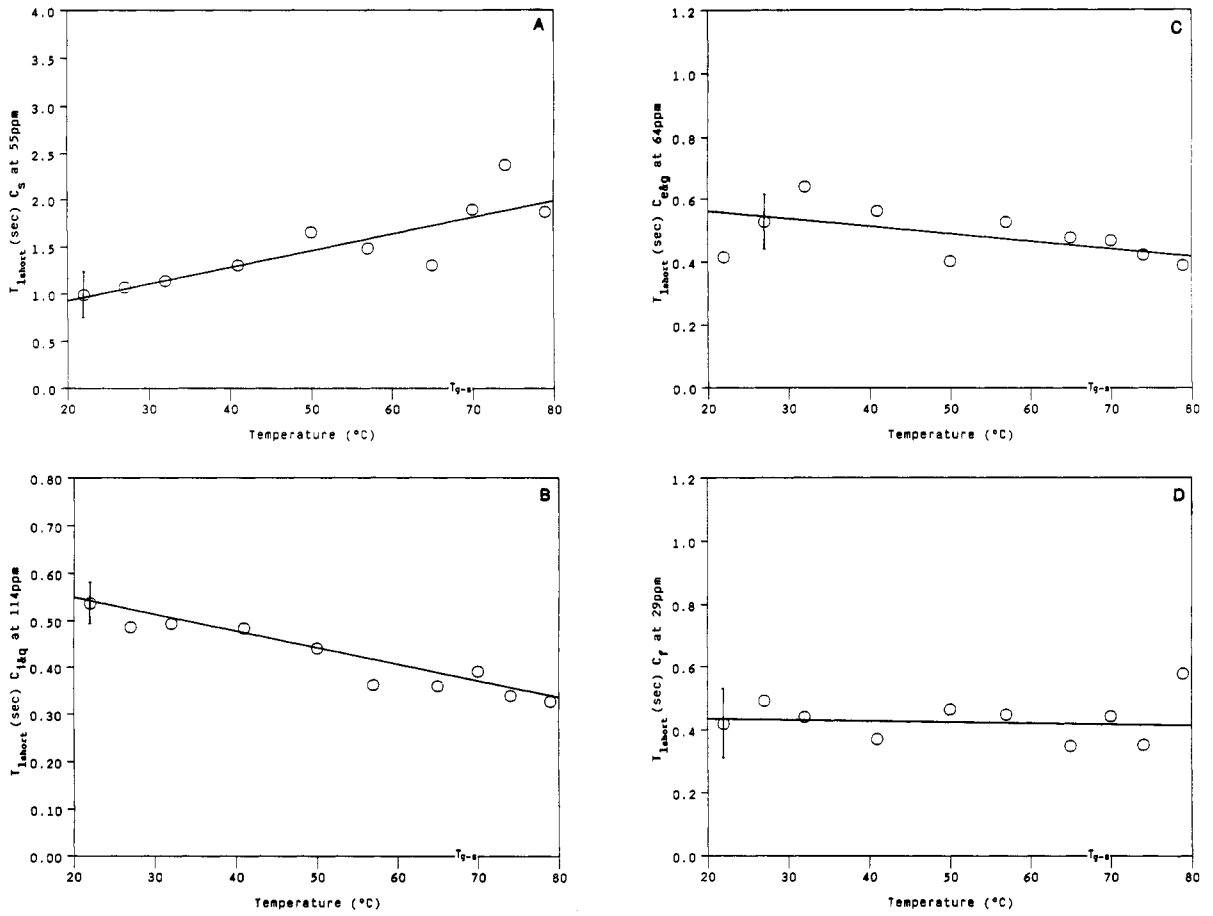

Figure 6. Plots of T_{1s} on an expanded scale for (A) the peak at 55 ppm assigned to C_s, (B) the peak at 114 ppm assigned to C_i and C_q, (C) the peak at 64 ppm assigned to C_e and C_g, and (D) the peak at 29 ppm assigned to C_f.

on the motion of a polymer due to the connectivity of the chain; there is a correlation between local conformations.[22] Consequently, the motion of a polymer is often highly anisotropic. Conformational jumps, corresponding to rotation of the C–H vector, must therefore be modeled based on damped rotation. Various models have been proposed for damped motion by specifying various forms of the autocorrelation function, which in turn specifies various forms of the spectral density. Dejean de la Batie et al.[22] present a review of several motional models. As a result of anisotropic motion, there is a distribution of correlation times that is centered about the mean correlation time. The use herein of eqs 11–13 is based on the simple assumption of random isotropic rotation and is valid to a first approximation. By assuming isotropic rotation, a single correlation time is determined.

The values of τ_c at 27 °C as calculated from eq 11 or eq 13 (as appropriate) are listed in the fourth column of Table III. These values are calculated from the values of T_{1s} listed in the fourth column of Table II. T_{1s} is used because it corresponds to relaxation via fluctuations of the dipolar interaction with bound protons. By considering only relaxation caused by fluctuations of the dipolar interactions with bound protons, the carbon to hydrogen bond distance can be substituted into eqs 11 and 13 for r_{C-H} (the internuclear distance), and the number of bound protons can be substituted for N (the number of dipolar interactions inducing relaxation).

Activation Energy for Reorientation. The theoretical temperature dependence of the rate of rotational motions is a simple Arrhenius expression

$$\tau_c = \tau_0 e^{E_a/RT} \tag{14}$$

where E_a is the activation energy for reorientation and R is the molar gas constant.[18] Thus, a plot of the natural logarithm of the correlation time as a function of the inverse temperature is linear with a slope that is proportional to the activation energy for motion. Figure 7 is such a plot for the protonated benzene carbons in the mesogen (C_i and C_q), the two outer methylene units of the spacer (C_e and C_g), and the center methylene unit of the spacer (C_f). The activation energies for these carbons, determined via curve fits of eq 14, are listed in Table IV.

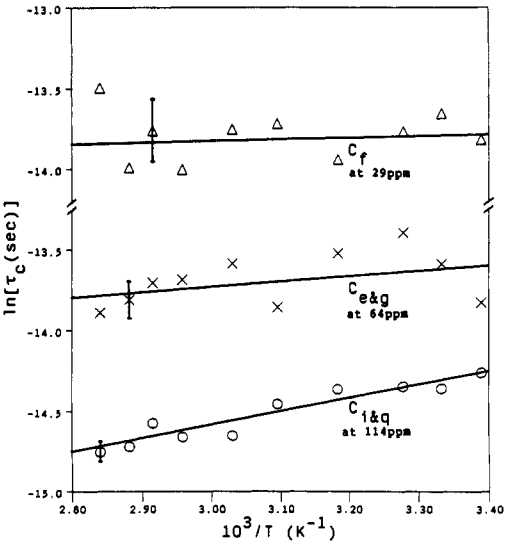

Figure 7. Arrhenius plot of the natural logarithm of the correlation time as a function of the inverse temperature for (○) the peak at 114 ppm assigned to C_i and C_q, (×) the peak at 64 ppm assigned to C_e and C_g, and (△) the peak at 29 ppm assigned to C_f.

Table IV
Activation Energies Calculated from Arrhenius Plots (Figure 7) of the Rotational Correlation Time as a Function of the Reciprocal Temperature[a]

	E_a,[b] J/mol
C_i and C_q 114 ppm	7.1×10^3
C_e and C_g 64 ppm	3.2×10^3
C_f 29 ppm	0.1×10^3

[a] The rotational correlation times were calculated from values of T_{1s} determined at 300 MHz in a cross-polarization-enhanced inversion–recovery pulse sequence. [b] Error: $\pm 0.6 \times 10^3$.

Table V
Values of T_{CH}, T_{CHs}, T_{CHl}, and $T_{1/2}$ at 36 °C for the PLC 4′-3-PMA Determined by a Cross-Polarization with Variable Contact Time Pulse Sequence at 300 MHz[a]

	T_{CH}, ms	$T_{1/2}$, ms
C_b 45 ppm	0.25	0.36
C_d 177 ppm	0.61	0.64
C_e and C_g 64 ppm	0.021 0.34	0.13
C_f 29 ppm	0.028 0.30	0.14
C_h and C_r 158 ppm	0.38	0.50
C_i and C_q 114 ppm	0.060 1.18	0.16
C_s 55 ppm	0.051 0.55	0.45

[a] Error: T_{CH}, ±0.02 ms; T_{CHs}, ±0.009 ms; T_{CHl}, ±0.05 ms; $T_{1/2}$, ±0.02 ms.

Note that C_i and C_q in the rigid mesogenic core have a very high E_a and that the spacer carbons α to the backbone and mesogen (C_e and C_g, respectively) also have a very high E_a. In contrast, the activation energy for the β spacer carbon (C_f) is nearly 2 orders of magnitude smaller.

Observation of Single/Double Exponentials for T_{CH}. Figure 3 is a typical plot of the magnetization in a variable contact time experiment (eq 5). Table V lists values of T_{CH} and $T_{1/2}$ at 36 °C for the various carbons.

A single T_{HH} is observed. Therefore, ^{1}H spin diffusion occurs. Although this is not conclusive proof, it does indicate that the PLC is likely composed of a single homogeneous phase to allow ^{1}H spin diffusion.[3,12] In this manner, T_{HH} is sensitive to domains larger than approximately 19 Å;[12] moreover, typical semicrystalline polymers have crystalline domain sizes in excess of 100 Å.

A single T_{CH} process is observed for each of the non-proton-bonded carbons, and two T_{CH}s are observed for each of the protonated carbons. Note in Table V that a single value of T_{CH} (indicating a single exponential) is listed for each of the non-proton-bonded carbons C_b, C_d, C_h, and C_r. Two T_{CH}s (indicating double exponentials) are listed in Table V for each of the protonated carbons C_e, C_g, C_f, C_i, C_q, and C_s.

Comparison of Relative $T_{1/2}$s. Table V lists values of $T_{1/2}$ at 36 °C for various carbons. Note that all of the non-proton-bonded carbons (C_b, C_d, C_h, and C_r) have long $T_{1/2}$s, and the proton-bonded carbons (C_e, C_f, C_g, C_i, and C_q) have much shorter $T_{1/2}$s. The transfer of magnetization from bound protons is more efficient than the transfer of magnetization from non-bonded protons. The transfer from bound protons is more efficient because the distance between the two interacting nuclei is smaller.

For the methylenic spacer carbons (C_e, C_f, and C_g) the values of $T_{1/2}$ can be directly compared to each other and related to mobility since each carbon has two bound protons. Note in Table V that the value of $T_{1/2}$ for the center methylene unit of the spacer (C_f) is equal to that for the outer methylenic units that are α to the backbone and α to the mesogen (C_e and C_g, respectively).

Temperature Dependence of T_{CH} and $T_{1/2}$. The values of T_{CH}, T_{CHs}, T_{CHl}, and $T_{1/2}$ were determined at several temperatures varying from 27 to 74.5 °C. For all of the carbons, no measurable trend was observed in any of these parameters as a function of temperature. Thus, in the Hz and kHz regimes, there is no significant change in mobility as the temperature is increased.

IV. Discussion

Cause of a Double Exponential for T_{CH}. A double exponential is observed for T_{CH} when the transfer of polarization occurs from bonded and nonbonded protons. The initial or fast process (T_{CHs}) is the transfer of magnetization from bound protons. The second or slow process (T_{CHl}) is the transfer of magnetization from nonbonded protons. The transfer of magnetization from bound protons is faster because this process is more efficient. The process is more efficient because the distance between the two interacting nuclei is smaller. That is, a bound proton is held a small distance (the bond length) from the polarizing carbon.

All nonprotonated carbons are single exponentials because the only process available is the transfer of magnetization from nonbonded protons. All protonated carbons are double exponentials because the transfer of magnetization occurs from bonded and nonbonded protons.

Double exponentials are commonly observed for the T_{CH} process for proton-bonded carbons in rigid organic solids.[5,13] The two T_{CH} processes correspond to the transfer of magnetization from tightly coupled and loosely coupled protons.[13] Certainly, a carbon can be considered tightly coupled to a bound proton. The initial process (T_{CHs}) is the coherent transfer of magnetization from a bound proton to its tightly coupled carbon.[13]

This is in complete analogy to the T_1 results where all non-proton-bonded carbons are single exponentials and all proton-bonded carbons are double exponentials. When two T_1s are observed the initial or fast process (with a short time constant, T_{1s}) is relaxation stimulated by fluctuations of the strong dipolar interaction with bonded protons. When two T_{CH}s are observed the initial or fast process (with a short time constant, T_{CHs}) is cross-polarization from bonded protons.

For T_1 and T_{CH}, x_s is the fraction of the component with a short time constant, the fraction of the process occurring with bonded protons. The values of x_s determined in the T_1 study and in the T_{CH} study are nearly equal. This suggests that the same mechanism is responsible for double exponentials for T_1 and T_{CH}.

Increase in Mobility with Temperature. As may be expected, the T_1 study shows a general trend toward an increased mobility at higher temperatures. The protonated benzene carbons in the mesogen (C_i and C_q) become more mobile at higher temperatures so the liquid crystalline core becomes more mobile with an increase in temperature. The methylene carbons in the spacer (C_e, C_g, and C_f) become more mobile at higher temperatures so the flexible free spacer becomes more mobile with an

increase in temperature. Thermal motions increase the mobility of the mesogen and the aliphatic spacer. The quaternary carbon in the backbone (C_b) becomes more mobile at higher temperatures so the main-chain backbone becomes more mobile with an increase in temperature. Main-chain viscosity decreases at higher temperatures.

The general trend toward an increase in mobility at higher temperatures is not surprising. Surely, a spin will be more mobile at a higher temperature as thermal motion increases. In fact, it could be said that T_1 for the methoxy carbon C_s increases with temperature because the motion is on the high-frequency side of the T_1 minimum and that T_1 decreases with temperature for C_i, C_q, C_e, C_g, C_f, and C_b because these motions are on the low-frequency side of the T_1 minimum. In this manner, the trend of T_1 as a function of temperature is often used to determine which side of the T_1 minimum a motion is on, without determining T_1 at two static magnetic fields.

The PLC can be expected to undergo motions on the slow side of the minimum because a PLC in the glassy state is extremely rigid (as can be seen by the large line widths). Highly mobile solid polymers such as elastomers may undergo motions on the fast side of the T_1 minimum.[23] On the slow side of the minimum, the trend toward smaller values of T_1 reverses as the temperature is increased, and progressively larger values of T_1 are observed when the T_1 minimum is passed.

Activation Energy for Reorientation. A high activation energy for motion indicates a high rigidity. The protonated benzene carbons in the mesogenic core (C_i and C_q) have a very high E_a; these carbons are part of the mesogenic core and are thus expected to be rigid. Conjugation causes benzene carbons to be very rigid, resulting in the observation of a high activation energy. The outer methylene carbons of the spacer (C_e and C_g) also have a very high E_a so these carbons are also rigid. These spacer carbons are rigid because they are α to the backbone and α to the mesogen, respectively. A high rigidity has been previously observed for the spacer carbon α to the mesogen in various other PLCs.[2,11] The activation energies, being a quantitative measure of rigidity, show that the rigidity of the α spacer carbon is nearly equal to that of the mesogen.

In contrast, the activation energy of the center methylene unit of the spacer (C_f) is nearly 2 orders of magnitude smaller. The center spacer carbon is extremely mobile in comparison. The center methylene unit of the spacer has the flexible property desired in an effective flexible free spacer. The function of the spacer in decoupling the motion of the mesogen from the motion of the backbone does not begin with the α spacer carbon but with the β spacer carbon.

Frequency Regime of Molecular Motions. The value of $T_{1/2}$ for the center methylene unit of the spacer (C_f) is equal to that for the outer methylenic units that are α to the backbone and α to the mesogen (C_e and C_g, respectively). Therefore, all three spacer carbons have equal mobilities as determined by cross-polarization dynamics.

Previous T_1 studies have shown that for many PLCs the spacer carbon α to the mesogen is more rigid than the β and subsequent spacer carbons.[2,11] In fact, for this particular PLC the T_1 results show that the rigidity of the α spacer carbon is quite high and nearly equal to that of the mesogen, whereas the β spacer carbon C_f is nearly 2 orders of magnitude more mobile.

The conclusions from the T_1 and $T_{1/2}$ experiments may seem contradictory upon first inspection, but they are not. T_{CH} is sensitive to molecular motions in the Hz and kHz regimes, and T_1 is sensitive to molecular motions in the MHz regime. Therefore, the two dynamic parameters are sensitive to different molecular motions.

Likewise, the T_1 results show interesting changes in mobility with temperature. The T_{CH} results show no significant change in mobility with temperature. Thus, the types of motions characteristic of this PLC are in the MHz regime, not in the Hz or kHz regimes.

V. Conclusions

In the glassy state, protonated carbons undergo spin–lattice relaxation stimulated by (A) fluctuations of the strong dipolar interaction with bonded protons and (B) simultaneous fluctuations of the weaker dipolar interaction with nonbonded protons. The result is the observation of two T_1s. Likewise, protonated carbons cross-polarize via the transfer of magnetization from bonded and nonbonded protons. The result is the observation of two T_{CH}s.

Within the glassy state the mobility of all local sites increases continuously with an increase in temperature due to thermal motion. This is evident in the temperature dependence of T_1. The mobility increases discontinuously at the glass to smectic transition.

A variable-temperature study of the cross-polarization dynamics shows no measurable trend in the relaxation parameters as a function of temperature. Therefore, in the Hz and kHz regimes of molecular motions, there is no significant change in the mobility of the PLC as the temperature is changed. In contrast, the MHz regime shows a continuous increase in mobility as the temperature is increased through the glass phase and a discontinuous increase in mobility at the glass to smectic transition.

Activation energies calculated from values of τ_c determined by a T_1 experiment show that the α spacer carbon is nearly as rigid as the mesogen. In contrast, the β spacer carbon is nearly 2 orders of magnitude more mobile. For molecular motions in the MHz regime the flexible free spacer does not function as "flexible" at the α spacer carbon, but begins to function as such at the β carbon.

At a given temperature, a comparison of the relative values of $T_{1/2}$ showed equal values for all of the methylenic spacer carbons. Therefore, in the Hz and kHz regimes of molecular motions, the mobilities of the methylenic spacer carbons are equal. Such low-frequency motions, corresponding to motions of large molecular groups, are surely averaged for the smaller atomic sites being observed. In contrast, the MHz regime shows a high rigidity for the spacer carbon α to the mesogen and a relatively high mobility for the β spacer carbon.

Both a comparison of the relative values of $T_{1/2}$ and a study of the cross-polarization dynamics as a function of temperature show no apparent differences in the mobility of a PLC in the Hz or kHz regimes, whereas in the MHz regime, both of these comparisons show differences in the mobility of this PLC. Therefore, the types of motions characteristic of this PLC occur in the MHz regime, not in the Hz or kHz regimes. Although motions with many frequencies occur simultaneously, of the motions studied only those motions in the MHz regime change significantly with temperature.

Within the wide range of motional frequencies that NMR is sensitive to, the Hz and kHz regimes are relatively low motional frequencies and the MHz regime is a relatively high motional frequency. Larger molecular groups undergo slow motions in the Hz and kHz regimes, and smaller molecular groups undergo fast motions in the MHz regime. Collective motions of entire groups of mesogens are typical of the types of motions that occur in the

Hz regime.[10] The overall rotation of an entire molecule is typical of the type of motion that occurs in the kHz regime.[9,10] Bond rotations and ring flips are typical of the types of motions that occur in the MHz regime.[9,10]

In conclusion, internal reorientations (such as trans–gauche isomerizations and ring flips) are the types of motions that are important in the dynamics of a PLC. After all, it is the lack of these motions that creates a rigid mesogenic core resulting in liquid crystallinity. The overall rotation of an entire molecule and the collective motion of an entire group of mesogens (motions such as bends, splays, and twists) are not the types of motions that cause liquid crystallinity; they are the result of liquid crystallinity.[9]

Acknowledgment. Special acknowledgment is given to Dr. Virgil Percec and Dimitris Tomazos from the Department of Macromolecular Science, Case Western Reserve University, for supplying the liquid crystalline polymer. Acknowledgment is given to the Materials Research Group and to the National Science Foundation for funding this research. Lastly, acknowledgment is given to Dr. W. Ritchey from the Department of Chemistry, Case Western Reserve University, and to Dr. J. B. Lando from the Department of Macromolecular Science, Case Western Reserve University, for aid in the preparation of this paper.

References and Notes

(1) Bovey, F. A.; Jelinski, L. W. *J. Phys. Chem.* **1985**, *89*, 571.
(2) Perry, B. C.; Koenig, J. L. *J. Appl. Polym. Sci., Appl. Polym. Symp.* **1989**, *43*, 165.
(3) Koenig, J. L. *Spectroscopy of Polymers*; American Chemical Society: Washington, DC, 1992.
(4) Torchia, D. A. *J. Magn. Reson.* **1978**, *30*, 613.
(5) Earl, W. L.; VanderHart, D. L. *Macromolecules* **1979**, *12*, 762.
(6) Veeman, W. S.; Menger, E. M.; Ritchey, W.; de Boer, E. *Macromolecules* **1979**, *12*, 924.
(7) Laupretre, F. *Prog. Polym. Sci.* **1990**, *15*, 425.
(8) Monnerie, L. *Pure Appl. Chem.* **1985**, *57*, 1563.
(9) Silvestri, R. L. M.S. Thesis, Case Western Reserve University, 1991.
(10) Müller, K.; Wassmer, K. H.; Kothe, G. *Adv. Polym. Sci.* **1990**, *95*, 1.
(11) Perry, B. C.; Hahn, B.; Percec, V.; Koenig, J. L. *Polymer* **1990**, *31*, 721.
(12) Grinsted, R. A.; Koenig, J. L. *J. Polym. Sci., Polym. Phys. Ed.* **1990**, *28*, 177.
(13) Lauprêtre, F.; Monnerie, L.; Virlet, J. *Macromolecules* **1984**, *17*, 1397.
(14) Schaefer, J.; Stejskal, E. O.; Buchdahl, R. *Macromolecules* **1977**, *10*, 384.
(15) Gerstein, B. C.; Dybowski, C. R. *Transient Techniques in NMR of Solids*; Academic Press: New York, 1985.
(16) Mehring, M. *Principles of High Resolution NMR in Solids*, 2nd ed.; Springer-Verlag: New York, 1983.
(17) Percec, V.; Tomazos, D. *Macromolecules* **1989**, *22*, 2062.
(18) Farrar, T. C. *An Introduction to Pulse NMR Spectroscopy*; Farragut Press: Chicago, 1989.
(19) Becker, E. D.; Fisk, C. L. *NMR in Living Systems*; Axenrod, T., Ceccarelli, G., Eds.; D. Reidel Publishing Co.: Boston, 1986.
(20) Hayamizu, K.; Yamamoto, O. *Bull. Chem. Soc. Jpn.* **1977**, *50*, 1295.
(21) Doddrell, D.; Glushko, V.; Allerhand, A. *J. Chem. Phys.* **1972**, *56*, 3683.
(22) Dejean de la Batie, R.; Lauprêtre, F.; Monnerie, L. *Macromolecules* **1988**, *21*, 2045.
(23) Andreis, M.; Liu, J.; Koenig, J. L. *Rubber Chem. Technol.* **1989**, *62*, 82.

Registry No. 4′-3-PMA (homopolymer), 118037-47-1.